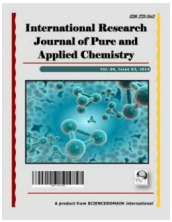

International Research Journal of Pure & Applied Chemistry
13(2): 1-14, 2016; Article no.IRJPAC.26191
ISSN: 2231-3443, NLM ID: 101647669

SCIENCEDOMAIN *international*
www.sciencedomain.org

Adsorption and Electrokinetic Properties of Catalase onto Perlite Samples

Özkan Demirbaş[1*] and M. Salih Nas[1]

[1]Department of Chemistry, Faculty of Science and Literature, University of Balikesir, 10145 Balikesir, Turkey.

Authors' contributions

This work was carried out in collaboration between both authors. Author ÖD designed the study, wrote the protocol and wrote the first draft of the manuscript. Author MSN performed the lab experiments, statistical analysis and managed the literature search. Both authors read and approved the final manuscript.

Article Information

DOI: 10.9734/IRJPAC/2016/26191
Editor(s):
(1) Bengi Uslu, Department of Analytical Chemistry, Ankara University, Ankara, Turkey.
Reviewers:
(1) Nurhidayatullaili Muhd Julkapli, University Malaya, Malaysia.
(2) Sinem Gokturk, Marmara University, Turkey.
Complete Peer review History: http://www.sciencedomain.org/review-history/17228

Original Research Article

Received 5th March 2016
Accepted 7th December 2016
Published 13th December 2016

ABSTRACT

With immobilized or adsorbed enzymes or protein, many improved features such as stability, reusability, continuous process, control of reactions, more favourable economic factors can be expected. For this purpose, in this study, the adsorption properties of casein onto some oxide minerals such as unexpanded (raw) (RP) and expanded (EP) perlite samples were studied. The expanded perlite is obtained from the raw perlite when it reaches temperatures of 850–900℃ (1,560–1,650℉). Raw perlite expands and softens after this heat treatment. The adsorption properties were studied as a function of concentrations of catalase, temperature, incubation time and pH of the aqueous solutions with both perlite samples. Similar experimental trends were found for the two perlite samples. According to the experimental results, the adsorption of catalase increases with increasing temperature and ionic strength of the solutions. The adsorption decreased with increasing pH. Maximum adsorption capacity values (q_m) showed dependence on pH. It was observed that q_e-pH curves reached a maximum at around neutral pH value. Furthermore, the electrokinetic properties of casein-covered oxide particles were also investigated

**Corresponding author: E-mail: ozkandemirbas@gmail.com;*

at similar conditions to those of the adsorption process. However, the adsorption capacity of expanded perlite is higher than the raw perlite due to the increase in surface area. The nature of the adsorption process was investigated using Langmuir and Freundlich isotherm models. Three kinetic models, the pseudo first-order, second-order and intraparticle diffusion, were used to predict the adsorption rate constants. The study of temperature effect has been quantified by calculating various thermodynamic parameters such as activation energy, Gibbs energy, enthalpy and entropy. In addition, activity of free and adsorbed catalase were studied and calculated the K_m and R_{max}.

Keywords: Adsorption; catalase; biocatalysis; electrokinetics; enzyme activity; biosorption.

1. INTRODUCTION

Adsorption of biomolecules are complicated processes in which the structural stability of a biomolecule, some physicochemical properties such as pH, ionic strength and temperature of the solution and surface properties of adsorbents are known to effect the affinity of a protein for a given interface. As most proteins adsorb with high affinity to hydrophobic surfaces, these proteins generally have less native structure than the same protein adsorbed on hydrophilic surfaces. It has also been seen that an increase in electrostatic interaction is generally accompanied by a reduction in the native structure [1-6].

As most proteins adsorb with high affinity to hydrophobic surfaces, these proteins generally have less native structure than the same protein adsorbed on hydrophilic surfaces. For this purpose, there are some studies concerned about protein adsorption onto some hydrophilic surface in the literature. However, understanding the interaction between the protein and the solid surface and assessing its effect on some applications is very important [7-9].

Catalase is a heme-containing redox enzyme known for its ability to degrade hydrogen peroxide (H_2O_2). Catalase is used in many areas of the industry such as textile, biosensor systems for peroxide and glucose [10-12]. Enzyme immobilization offers advantages over free enzymes in choice of batch or continuous processes, rapid termination of reactions, controlled product formation, ease of enzyme removal from the reaction mixture and adaptability to various engineering designs [13,4,5]. In the immobilization techniques adsorption have a higher commercial potential than the other methods, because adsorption is simpler and less expensive and a high catalytic activity can be retained. Adsorption method also offers the reusability of expensive supports after inactivation of immobilized enzyme [6-9]. In general, this method requires a large surface area to be sufficiently accurate. Otherwise, various techniques such as depletion [14], quartz crystal microbalance (QCM) [15], enzyme-linked immunosorbent assay (ELISA) [16], ellipsometry [17], total internal reflection fluorescence (TIRF) [18], neutron reflection [19], fourier transform infrared spectroscopy (FTIR) [20], fluorescence spectroscopy [21] and atomic force microscopy (AFM) [22] have been used to measure the amount of adsorbed proteins on solid surfaces.

Some materials such as porous glass, silica gels and cellulose are used for preparation of immobilized enzymes [10,11]. Table 1 shows some typical proteins adsorbed on surfaces of different solid materials.

In this study, the adsorption properties of casein onto some oxide minerals such as expanded (EP) and unexpanded (raw) perlite (RP) samples were investigated as a function of concentrations, temperature, incubation time and pH. Furthermore, some parameters of kinetics and thermodynamics and catalase activities onto surfaces were investigated.

Table 1. Some protein adsorbed on different solid surfaces

Protein	Solid surface	Method	Ref.
α-Lactoalbumin	Silica gel and hematite	Depletion	[23]
Ferritin	Gold	Quartz crystal micro (Q.C.M)	[24]
Egg white lysozyme	Silicon oxide	Ellipsometry	[25]
β-Casein and catalase	Kaolinite	Depletion	[26]
BSA	Polystrene, stainless steel and some oxides	Depletion, RI method	[14,27]

2. MATERIALS AND METHODS

Catalase from bovine liver was purchased from Sigma-Aldrich Co. The perlite samples were purchased from İzmir, Turkey. The chemical composition of the perlite was determined as SiO_2:73.55, Al_2O_3:12.49, CaO:1.03, Fe_2O_3:0.55, Na_2O:1.55, K_2O:3.35, MgO:0.35, LoI (loss of ignition):7.13 by XRF. Perlite samples were treated before using in the experiments as follows [14]. All chemicals used were of analytical grade.

The results obtained of the cation exchange capacity (CEC), the density and the specific surface area of the perlite samples are measured as CEC (meq/100 g): 25.90 and 33.40, particle diameter (µm): -75.0, pH of 3% aqueous solution: 7.09 and 7.07, density (g mL^{-1}): 2.30 and 2.24 and specific surface area (m^2 g^{-1}). 12.23 and 14.55 for RP and EP, respectively.

2.1 Zeta Potential

In this study, a Zeta Meter 3.0 was used to measure the zeta potentials of the suspensions prepared [28]. The Zeta Meter 3.0 device calculates the zeta potential using the Smoluchowski equation as follows [28]:

$$\zeta = 4\pi V_t E/D \quad (1)$$

To measure the zeta potential, the suspensions were prepared as follows: the perlite samples were added to 250 mL polymer bottle in which 100 mL of a suspension was transferred yielding final perlite concentrations of 3 g L^{-1} for RP and EP. And then, the suspensions were shaken by a thermostatic shaker bath. The suspensions after 24 h were taken from the bath to stand for 5 min to allow larger particles settle. About 10 mL suspension taken from the bottle and was measured the zeta potentials. The voltage applied in measuring the zeta potentials was between 50 and 150 mV.

2.2 Adsorption Experiments

In this study, to recognize the catalase adsorption phenomenon on the perlite surface, some experimental effects such as concentrations of biomolecule, pHs (3–10), constant ionic strength and sodium phosphate buffer concentration on adsorption for 24 h at 22℃ were selected. The suspensions were centrifuged for 10 min at 3000 rpm after 24 h and then the concentrations of the residual enzyme, Ce, were measured by Bradford method [29]. The amounts of enzyme adsorbed were calculated from the concentrations in suspensions before and after adsorption process.

2.3 Activity of Enzyme

The activity of enzyme was measured photometrically by direct measurement of the decrease in the absorbance of H_2O_2 at 230 nanometer. H_2O_2 solutions (0.004 – 0.200 M) were used to determine the activity. 0.3 g of enzyme adsorbed perlite particles were mixed with H_2O_2 solution in 0.020 M phosphate buffer (pH 7.0) at 22℃. The values of absorbance of the constituents were measured and the some kinetic parameters of adsorbed enzyme, K_m (Michaelis constant) and V_{max} (maximum reaction rate) for adsorbed and free enzyme on perlite samples were determined by varying the concentration of H_2O_2 in the reaction medium.

3. RESULTS AND DISCUSSION

3.1 Isoelectric Point (IEP) of Samples

Clays and oxide minerals have usually one ionisable group on surfaces. They may be a proton or hydroxyl ion depending on the pH of the medium [30]. These ionizations are given as follows;

$$SO\text{-}H + H^+ \rightleftharpoons SOH_2^+ \quad (2)$$

$$SO\text{-}H + OH^- \rightleftharpoons SO^- + H_2O \quad (3)$$

at isoelectric point (IEP),

$$[SOH_2^+] = [SO^-] \quad (4)$$

where ‘‘S’’ denotes the surface.

The net charge on the enzyme or solid surface at the isoelectric point is zero. The pH value at the isoelectric point is indicated by pH_{iep}. The pH_{iep} of the RP and EP were indicated by measuring the zeta potential as a function of suspension pH (Fig. 1). So both perlite samples have no isoelectric points in this studied pH range. As sees in Fig. 1, the increase of the suspension pH results in an increase in the negative charge of the oxide minerals.

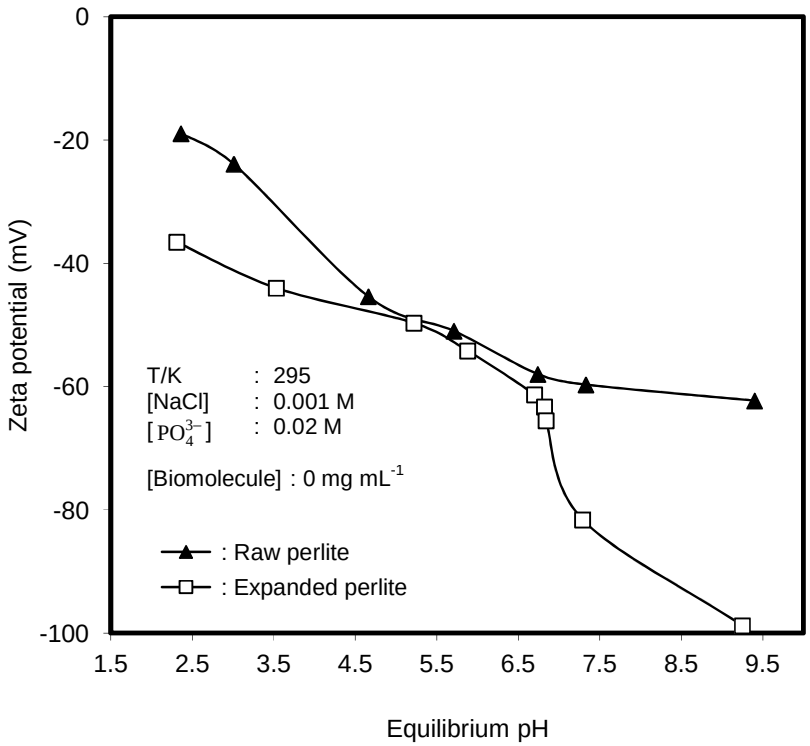

Fig. 1. The change of the zeta potential with equilibrium pH of the RP and EP

3.2 Adsorption Amounts of Perlites as a Function of Incubation Time and Temperature

Experimental conditions such as 0.001 M NaCl, 0.02 M phosphate ions at pH 7.0 were adjusted in the adsorption experiments. The experimental results and some conditions are given in Fig. 2. The time required to reach a constant concentration in Fig. 2 is about 4 hours.

The degree of adsorption depends on the temperature of the solid–liquid interface. The rates of adsorption were studied in the temperature range of 295 and 315 K. The effect of temperature on the adsorption is shown in Fig. 2. According to the Fig. 2, it is observed that at

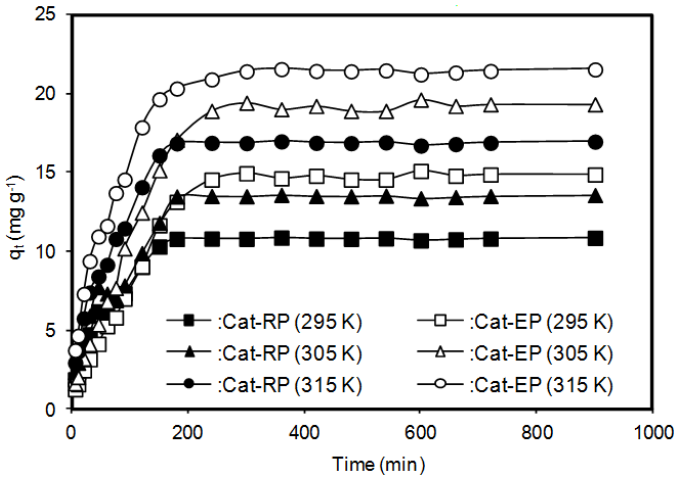

Fig. 2. The adsorption of enzyme onto RP and EP as a function of temperature. (Experimental conditions: [Catalase]: 1 mg mL^{-1}, [PO_4^{3-}]: 0.02 M, [NaCl]: 0.001 M and pH 7)

higher temperatures the adsorption is higher, and the adsorption process was endothermic process. This result can be explained as follows: (i) the adsorption process of catalase onto perlite surface is endothermic, this result indicates that the process is entropically driven (ii) it can be explained that with increasing temperature, the number of biomolecules penetrating into the pores of the adsorbent is also increasing [14,30].

3.3 Zeta (ζ) - Potential Values of Adsorbed Catalase on Perlite Samples

Experiments on the determination of zeta potentials and experiments on the adsorption were carried out under the same experimental conditions. In this case, the adsorption potential of the samples is related to the zeta potentials of

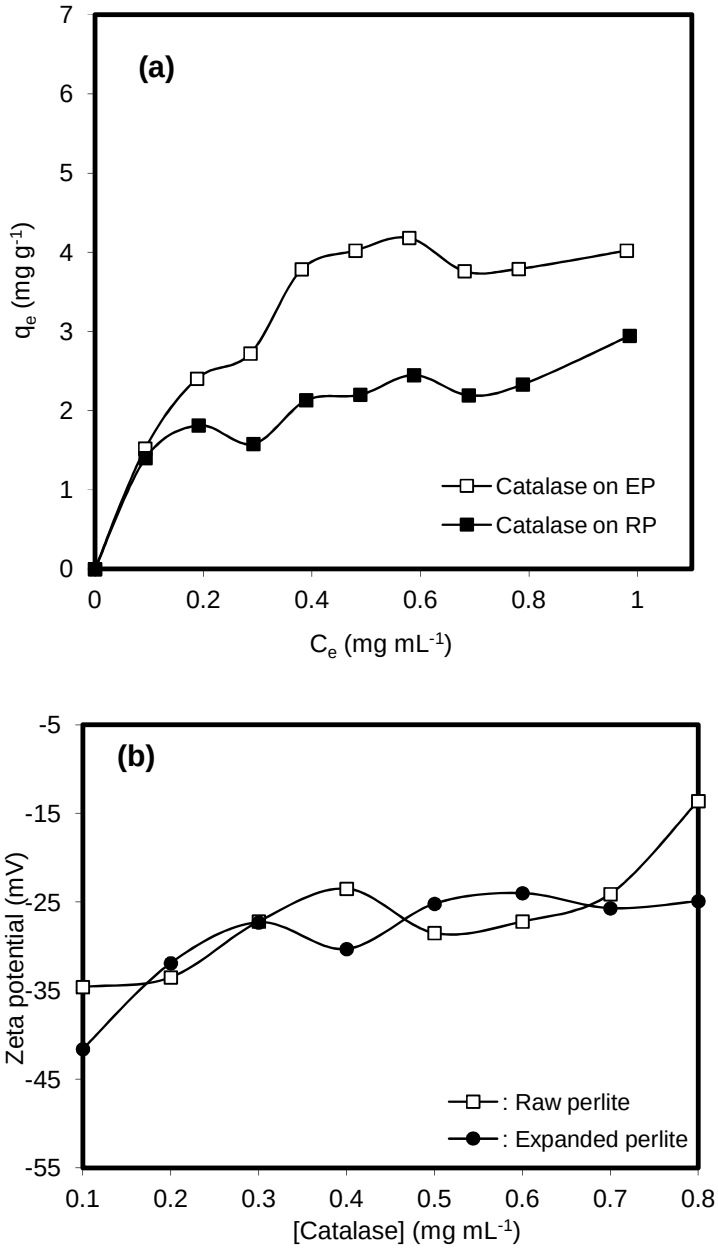

Fig. 3. (a) The variation of adsorption isotherms, and (b) change of the zeta potential with different initial catalase concentrations of perlite samples in the suspensions. (Experimental conditions:[PO_4^{3-}]: 0.02 M, [NaCl]: 1 mM, pH 7, 295 K)

the minerals. The adsorption isotherms of catalase and the zeta potential of minerals in the suspension were given in Fig. 3(a) and (b), respectively. From the figures, it is observed that the adsorption capacity of perlite increases as the initial concentration of catalase increases. However, increasing the initial enzyme concentration reduces the zeta potential of minerals. Increasing the concentration of catalase on the perlite leads to a reduction in the zeta potential of the catalase adsorbed particles but not positive at pH 7.0. Similar result was given in our previous paper [14]. Fig. 4(a) shows the catalase adsorption onto perlite surface and Fig. 4(b) shows the change of the zeta potential with the equilibrium pH of the suspensions. As can be seen from Fig. 4(a), the adsorption capacity of catalase onto perlite surface is the highest at around pH 6. This pH value is close to the isoelectric point of the catalase. The pH values of the suspensions have a very significant effect on the adsorption of biomolecules on solid surfaces [14,31]. Catalase has a negative net charge in solutions having a pH greater than 6.0. Electrostatic repulsion between the perlite surface and catalase in these solutions may cause a decrease in the adsorption of the catalase in the pH range of 6-10.

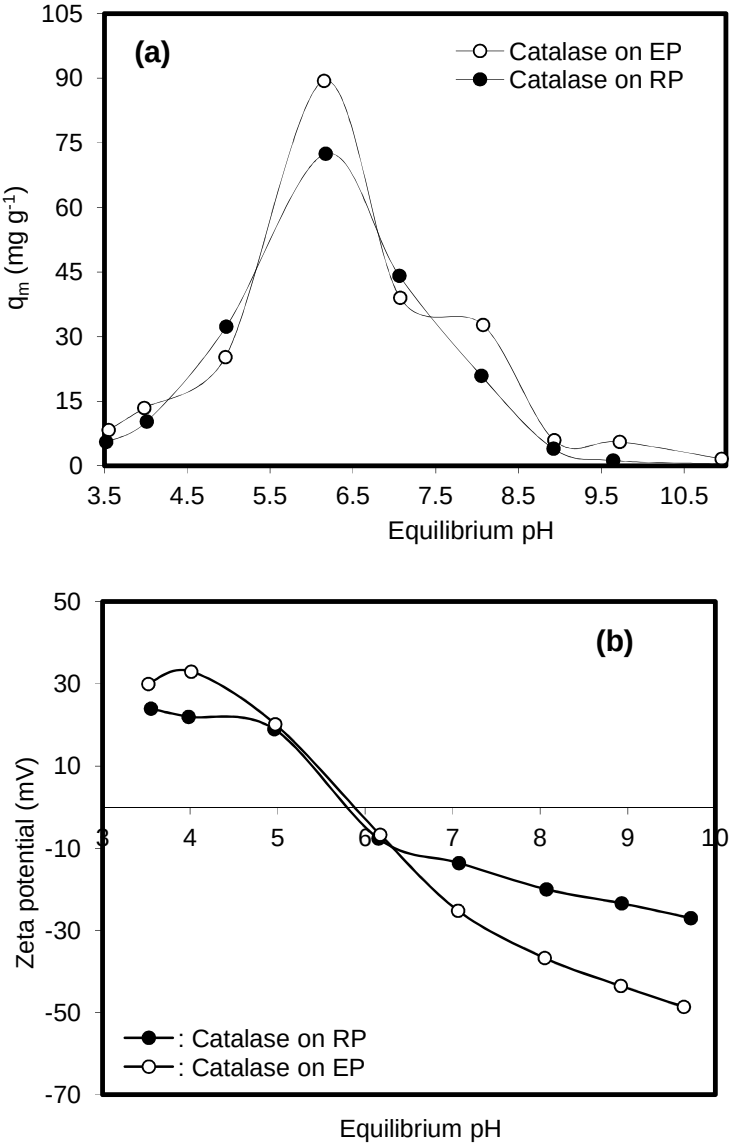

Fig. 4. (a) Adsorption of enzyme and (b) the variation of zeta potential of solid suspensions. (Experimental conditions: 295 K, $[PO_4^{3-}]$: 0.02 M, [NaCl]: 0.001 M, [Catalase]:1mg ml^{-1})

The addition of proteins to suspensions significantly affects the zeta potential of the suspended particles [32-35].

Adsorptions of catalase onto RP and EP have caused a change in the zeta potential and shifted the isoelectrical point of the oxide minerals from approximately 5.7 for perlite samples; which is the isoelectrical point of catalase in the solution.

3.4 Effect of Temperature on Catalase Adsorption onto Perlite

In the present study, the temperature range was taken as 15-45℃ to investigate the effect of temperature on adsorption. Fig. 5(a) and 5(b) illustrate the catalase adsorption onto raw and expanded perlite surface, respectively, at different temperature. From both Figures, it is observed that the increase of temperature increases the concentration of catalase which adsorbs to the surface of perlite samples. This observation can be explained as described in the Section 3.2. The amount of catalase adsorbed on the surface of perlite samples has a positive relationship with temperature and adsorption process is endothermic. In addition, the constants of Langmuir and Freundlich adsorption isotherms can be calculated by using these figures and experimental data.

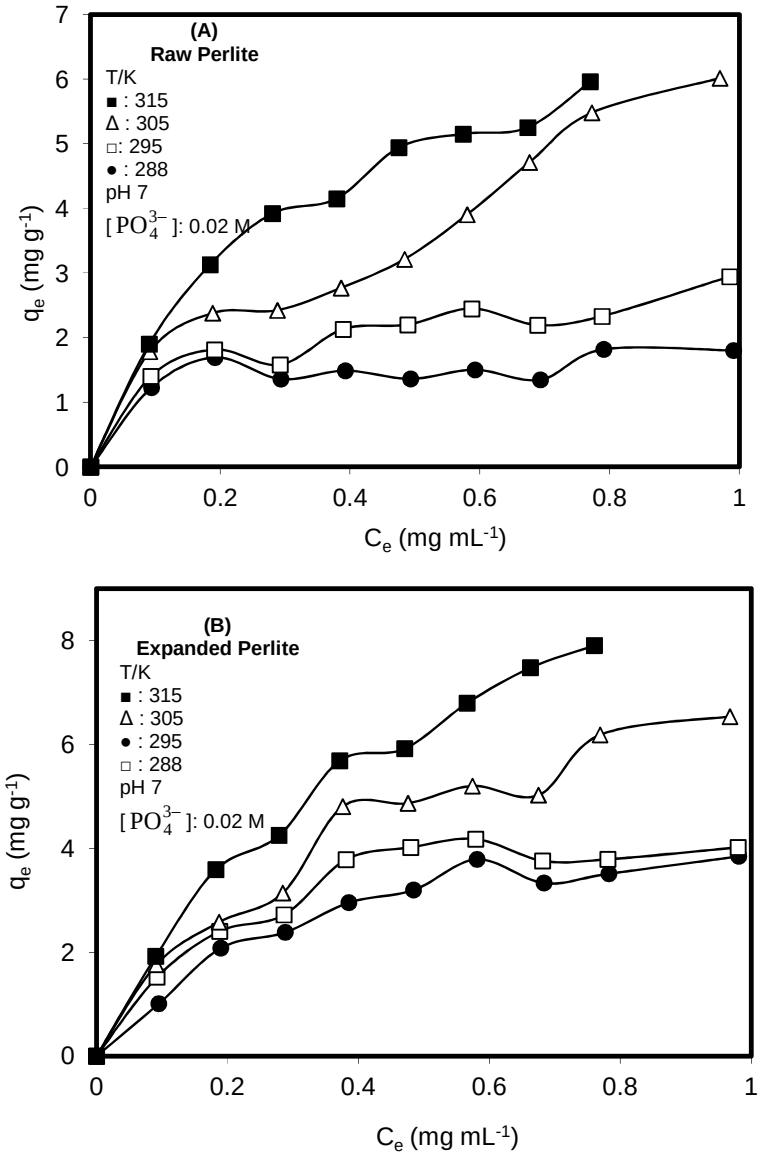

Fig. 5 (a and b). The effect of temperature for catalase adsorption on perlite samples

3.5 Analysis of FTIR Spectra

The Fourier transform infrared (FTIR) spectra were carried on a spectrophotometer (Perkin Elmer) at room temperature and the samples were prepared in pellet form using spectroscopic grade KBr. To examine the nature of the interaction between the catalase and perlites (RP and EP), FTIR spectra of perlites, catalase and adsorbed catalase were obtained. The spectrums were shown in Fig. 6. FTIR spectra results of catalase showed strong peaks at v =1620–1680 cm^{-1} and v = 1480–1580 cm^{-1}, mainly associated with amide-I and amide-II stretching vibration bands, respectively [36,37]. IR spectra obtained for biomolecule adsorbed on perlite samples show the peaks of the amide I band at about 1655 cm^{-1} and amide II band at about 1529 cm^{-1}, which are typical of biomolecules [37].

3.6 Adsorption Isotherms

3.6.1 Langmuir adsorption isotherm

The Langmuir adsorption isotherm describes a single layer deposition on a homogeneous surface. For this reason, equilibrium is the most important sign in adsorption process. According to the Langmuir theory, when the adsorption process reaches equilibrium, the adsorbent surface adsorbs the maximum amount of substance.

The equation for the Langmuir isotherm is shown below [38]. With this equation, isotherm graphs can be plotted and the constants of Langmuir equation are calculated.

$$\frac{C_e}{q_e} = \frac{1}{q_m K} + \frac{C_e}{q_m} \quad (5)$$

where C_e (mg mL^{-1}) is the concentration of catalase in the liquid phase of the suspension at equilibrium time. q_e (mg g^{-1}) is the concentration of catalase adsorbed onto perlite surface, K is Langmuir constant and at the same time it refers to the equilibrium constant, and q_m is the monolayer capacity of the adsorption. The Langmuir constants can be calculated from the slope and intercept of the linear graph using Eq. 5. However, Table 2 shows that the correlation values of the Langmuir isotherm plots are not sufficient to explain the adsorption phenomenon through this theory.

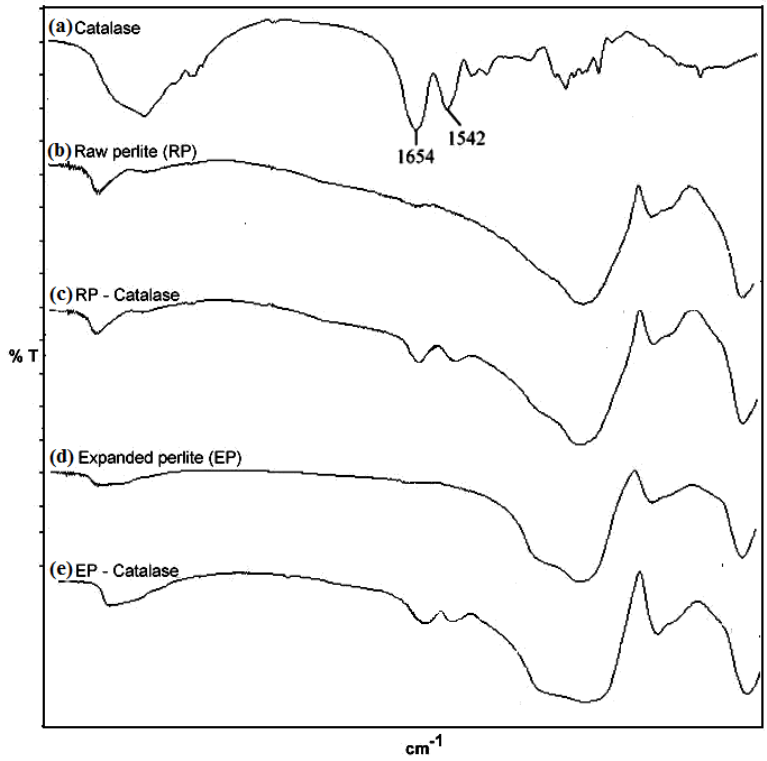

Fig. 6. FTIR spectra of (a) catalase, (b) raw perlite, (c) catalase adsorbed raw perlite, (d) expanded perlite and (e) catalase adsorbed expanded perlite

Table 2. Isotherm constants for adsorption of biomolecules on perlite samples

Sample	(*T*/K)	Freundlich isotherm parameters			Langmuir isotherm parameters		
		n	K_F	R^2	q_m (mg g^{-1})	K (L mg^{-1})	R^2
Catalase-RP	288	2.88	1.77	0.98	1.82	12.22	0.93
	295	3.33	2.86	0.99	3.13	5.42	0.92
	305	1.96	5.81	0.99	10.00	1.39	0.70
	315	1.99	6.82	0.98	8.33	3.23	0.98
Catalase-EP	288	3.11	2.11	0.97	2.02	13.25	0.85
	295	2.97	3.55	0.98	4.55	8.21	0.92
	305	2.01	9.12	0.98	9.88	4.32	0.73
	315	1.85	10.87	0.97	11.22	2.45	0.82

(Experimental cond. pH 7, $[PO_4^{3-}]$: 0.02 M, [NaCl]: 0.001 M)

3.6.2 Freundlich adsorption isotherm

The equation for the Freundlich adsorption isotherm is an empirical exponential equation as follows [39]:

$$q_e = K_F C_e^{1/n} \quad (6)$$

According to the equation, as the concentration of adsorbate in the aqueous medium increases, the amount of adsorbed on the surface also increases. Therefore, according to this theory adsorption will always continue as the adsorbate is added to the aqueous medium.

The linear form of Equation 6 can be written as:

$$\ln q_e = \ln K_F + \frac{1}{n} \ln C_e \quad (7)$$

where K_F and n are the Freundlich isotherm constants. In the Freundlich theory, adsorption is mostly described by heterogeneity. The constant n in the Eq. 7 also characterizes heterogeneity which means that the surface is too heterogeneous if its value is close to zero. K_F, one of the Freundlich constants in the Eq. 7, is also related to binding energy.

K_F and n constants were calculated from the linear graph of lnC_e versus lnq_e in Equation 7 and the results are given in Table 2. As Table 2 shows, the correlation coefficient of the linear graph of the Freundlich isotherm is in the range of 0.97-0.99, so the experimental data in this study are in agreement with the Freundlich isotherm.

3.7 Adsorption Kinetics

In order to better understand the controlling mechanism of the adsorption of catalase onto perlite surface, some kinetic models were investigated. Some of these are described below.

3.7.1 Pseudo-first-order equation

The pseudo-first-order equation is shown in the literature as follows [40]:

$$\ln(q_e - q_t) = \ln q_e - k_1 t \quad (8)$$

q_e and q_t, (mg g^{-1}), shown in Equation 8, indicate quantities of adsorbed catalase at equilibrium and time t, respectively. k_1 is the rate constant (min^{-1}).

$t_{1/2}$ is the time (min) for half-adsorption of catalase onto perlite samples and is calculated by the following equation.

$$t_{1/2} = \frac{\ln 2}{k_1} \quad (9)$$

The values of k_1 and $t_{1/2}$ calculated by using Eq. 8 and 9 are given in Table 3.

3.7.2 Pseudo-second-order equation

The pseudo-second-order equation is shown in the literature as follows [41]:

$$\frac{t}{q_t} = \frac{1}{k_2 q_e^2} + \frac{1}{q_e} t \quad (10)$$

q_e and q_t , (mg g^{-1}), shown in Equation 10, indicate quantities of adsorbed catalase at equilibrium and time t, respectively. k_2 is the rate constant (g(mg min)$^{-1}$).

$t_{1/2}$ is the time (min) for half-adsorption of catalase onto perlite samples and is calculated by the following equation.

$$t_{1/2} = \frac{1}{k_2 q_e} \quad (11)$$

The values of k_2 and $t_{1/2}$ calculated by using Eq. 10 and 11 are given in Table 3.

Table 3. Kinetic values calculated for catalase adsorption on perlite samples

Sample	(*T*/K)	First-order kinetic equation				Second-order kinetic equation				Intraparticle diffusion equation			
		$k_1 x10^3$ (min^{-1})	q_e (calculated) mg g^{-1}	R^2	$t_{1/2}$ (min)	$k_2 x10^3$ g (mg min)$^{-1}$	q_e (calculated) mg g^{-1}	R^2	$t_{1/2}$ (min)	$k_{int(1)}$ mg (g $min^{1/2})^{-1}$	R^2	$k_{int(2)}$ mg (g $min^{1/2})^{-1}$	R^2
Catalase – RP	295	19.9	11.11	0.91	34.8	2.64	11.40	0.99	33.17	0.81	0.93	0.031	0.50
Catalase – RP	305	18.4	15.79	0.87	37.6	1.70	14.40	0.99	40.89	0.86	0.93	0.022	0.76
Catalase – RP	315	18.9	18.08	0.92	36.7	1.62	17.85	0.99	34.45	1.28	0.88	0.014	0.45
Catalase – EP	295	13.7	19.29	0.95	50.6	0.57	17.33	0.99	101.03	0.98	0.95	0.010	0.67
Catalase – EP	305	19.7	36.59	0.86	35.2	0.46	22.42	0.99	97.07	1.34	0.95	0.015	0.56
Catalase – EP	315	15.1	21.32	0.97	45.9	1.22	22.72	0.99	35.89	1.58	0.92	0.012	0.55

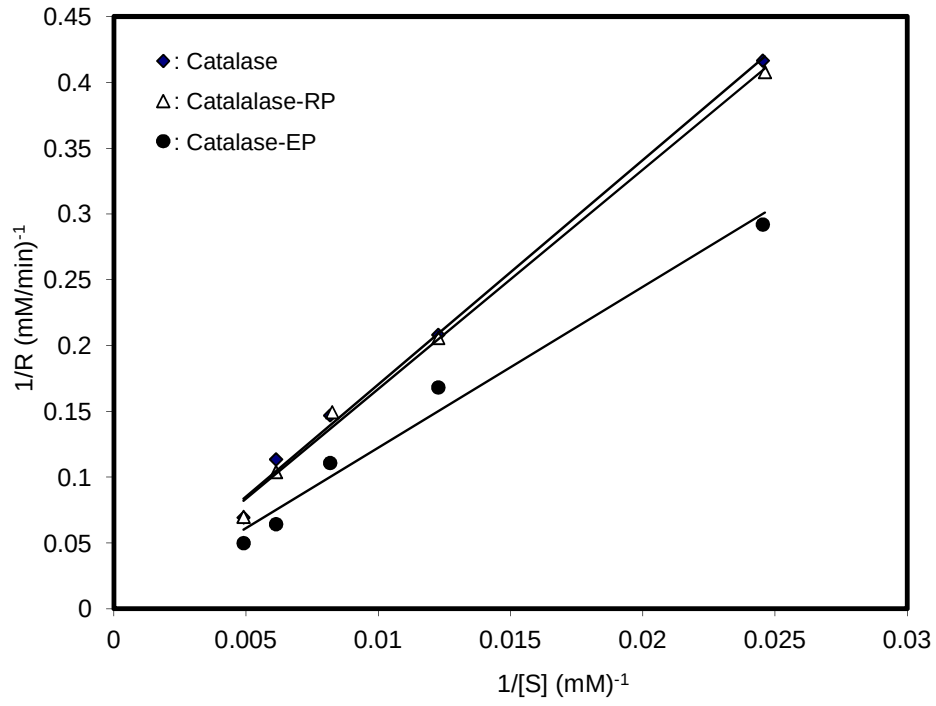

Fig. 7. Lineweaver-Burk plot of pure and adsorbed catalase

3.7.3 Intraparticle diffusion

According to a function of $(D_t/r^2)^{1/2}$, the fractional representation of the diffusion coefficient, D_t, of the solute molecules into the particle having radius r is as follows:

$$q_t = f(\sqrt{t}) \tag{12}$$

The initial rate equation for intraparticle diffusion is as follows [14,30]:

$$q_t = k_{\text{int}}\sqrt{t} + C \tag{13}$$

From the eq. 13, the intraparticle diffusion rate constant from the slope is calculated from the linear graph of the q_t against $t^{1/2}$. Calculated k_{int} values are given in Table 3.

3.8 Thermodynamic Parameters

The activation energy E_a can be calculated from the following Arrhenius equation using the k2 constants calculated from the second order kinetic equation:

$$\ln k_2 = \ln A - \frac{E_a}{R_g T} \tag{14}$$

From the linear graph of $\ln k_2$ versus 1 / T, the activation energy, E_a, from the slope and the Arrhenius factor, A, from intercept value of graph can be calculated.

Free energy (ΔG*), enthalpy (ΔH*) and entropy (ΔS*) of activation can be calculated by Eyring equation [42]:

$$\ln\left(\frac{k_2}{T}\right) = \ln\left(\frac{k_b}{h}\right) + \frac{\Delta S^*}{R_g} - \frac{\Delta H^*}{R_g T} \tag{15}$$

where k_b and h are Boltzmann's and Planck's constants, respectively. According to Eq. (15), a plot of $\ln(k_2/T)$ versus 1/T should be a straight line with a slope $-\Delta H^*/R_g$ and intercept $[\ln(k_b/h) + \Delta S^*/R_g]$. ΔH* and ΔS* were calculated from slope and intercept of line, respectively. Gibbs energy of activation may be written in terms of entropy and enthalpy of activation:

$$\Delta G^* = \Delta H^* - T\Delta S^* \tag{16}$$

ΔG* was calculated at 295 K from Eq. (16).

As a result, the thermodynamics parameters of catalase on perlite samples were calculated as

E_a (kjmol^{-1}): 29.16 and 33.12, ΔG^*(kjmol^{-1}): 215.2 and 175.6, ΔH^*(kjmol^{-1}): 35.02 and 38.55 and ΔS^*(jmol^{-1}K^{-1}): -611.5 and -595.1 for RP and EP, respectively.

3.9 Kinetic Parameters of Catalase

K_M and $R_{\max}$ are characteristic constants for enzymes. Equation for calculating K_M and $R_{\max}$ is below and derived from the Michaelis-Menten equation [43]:

$$\frac{1}{R} = \frac{K_M}{R_{\max}} \frac{1}{[S]} + \frac{1}{R_{\max}} \quad (17)$$

The linear graph plotted against $\frac{1}{R}$ versus $\frac{1}{[S]}$ is known as the Lineweaver-Burk plot (see Fig. 7). The slope of this graph is equal to $\frac{K_M}{R_{\max}}$ value and intercept is equal to $\frac{1}{R_{\max}}$.

In this study, from the experimental data, K_M and $R_{\max}$ and $\frac{R_{\max}}{K_M}$, called catalytic efficiency of adsorbed and pure catalase are calculated as K_m (mM): 172.09, 61.08 and 75.77, R_{max} (mM min^{-1}) : 10.10, 5.00 and 4.54, R_{max} / K_m (min^{-1}): 0.058, 0.082 and 0.060 for pure catalase, EP and RP, respectively. As seen from results, the K_m and R_{max} values of the adsorbed enzyme are lower than pure enzyme.

4. CONCLUSIONS

- The zeta potential values weren't 0 mV for both perlite samples in this studied pH range of 1.5–10.
- The adsorbed catalase on perlites has negative charge at pH 7.0. The q_m values for catalase adsorption are maximum at about pH 6, which is near to the iep of catalase,
- Catalase has a negative net charge in solutions having a pH greater than 6.0. Electrostatic repulsion between the perlite surface and catalase in these solutions may cause a decrease in the adsorption of the catalase in the pH range of 6-10.
- Adsorptions of catalase onto RP and EP have caused a change in the ζ-potential and shifted the isoelectrical point of the oxide minerals from approximately 5.7 for perlites; which is the isoelectrical point of catalase in the solution.
- The adsorption process becomes more favourable with increasing temperature,
- FTIR spectra obtained for catalase adsorbed on perlites show the peaks of the amide I band at about 1655 cm^{-1} and amide II band at about 1529 cm^{-1}, which are typical for biomolecules,
- The Freundlich model yields a much better fit than the Langmuir model.
- Kinetic studies indicated that the adsorption follows pseudo-second-order kinetic equation.
- Thermodynamical parameters were also evaluated for the catalase-adsorbent systems and revealed that the adsorption process was endothermic in nature.
- The K_m and R_{max} values of the adsorbed enzyme are lower than pure enzyme.

ACKNOWLEDGEMENTS

The author acknowledges support from the BAP-2015-0001 (Tracking No: 1.2014.0071), the University of Balikesir.

COMPETING INTERESTS

Authors have declared that no competing interests exist.

REFERENCES

1. Giacomelli CE, Norde W. The Adsorption–Desorption Cycle. Reversibility of the BSA–Silica System. J. Colloid Interf. Sci. 2001;233:234–240.
2. Norde W. In: Baszkin A, Norde W, (Eds.), Physical chemistry of biological interfaces, Marcel Dekker Inc. New York. 2000;115.
3. Arica MY, Soydogan H, Bayramoglu G. Reversible immobilization of Candida rugosa lipase on fibrous polymer grafted and sulfonated p(HEMA/EGDMA) beads. Bioprocess. Biosyst. Eng. 2010;33:227–236.
4. Karagoz B, Bayramoglu G, Altintas B, Bicak N, Arica MY. Poly (glycidylmethacrylate)-polystyrene diblocks copolymer grafted nanocomposite microspheres from surface-initiated atom transfer radical polymerization for lipase immobilization: Application in flavor ester

synthesis. Ind. Eng. Chem. Res. 2010; 49:9655–9665.
5. Nakanishi K, Sakiyama T, Imamura K. On the adsorption of proteins on solid surfaces, a common but very complicated phenomenon. J. Biosci. Bioeng. 2001;91: 233-244.
6. Luo Q, Andrade JD. Cooperative adsorption of proteins onto hydroxyapatite. J. Colloid and Interface Sci. 1998;200:104-113.
7. Kondo A, Murakami F, Higashitani K, Circular dichroism studies on conformational changes in protein molecules upon adsorption on ultrafine polystyrene particles. Biotechnol. Bioeng. 1992;40889-984.
8. Kondo A, Oku S, Murakami F, Higashitani K. Conformational changes in protein molecules upon adsorption on ultrafine particles. Colloids Surf. B: Biointerf. 1993;1:197.
9. Buijs J, Norde W, Lichtenbelt JWT, Changes in the secondary structures of adsorbed IgG and (Fab)2 studied by FTIR spetroscopy. Langmuir. 1996;12:1605-1613.
10. Horst F, Rueda EH, Ferreira ML. Activity of magnetite-immobilized catalase in hydrogen peroxide decomposition. Enzyme Microb. Technol. 2006;38(7): 1005–1012.
11. Domink Jürgen-Lohmann L, Raymond Legge L, Immobilization of bovine catalase in sol–gels. Enzyme Microb. Technol. 2006;39(4):626–633.
12. Yoshimoto M, Sakamoto H, Yoshimoto N, Kuboi R, Nakao K. Stabilization of quaternary structure and activity of bovine liver catalase through encapsulation in liposomes. Enzyme Microb. Technol. 2007; 41:849–858.
13. Kennedy JF, Melo EHM, Jumel K, Immobilized enzymes and cells. Chem. Eng. Prog. 1990;45:81-89.
14. Alkan M, Demirbas O, Dogan M, Arslan O, Surface properties of bovine serum albumin – adsorbed oxides: Adsorption, adsorption kinetics and electrokinetic properties. Microporous Mesoporous Mater. 2006;96:331–340.
15. Caruso F, Rodda E, Furlong DN. Orientational aspects of antibody immobilization and immunological activity on quartz crystal microbalanee electrodes. J. Colloid Interface Sci. 1996; 178:104-115.
16. Stevens PW, Hansberry MR, Kelso DM, Assessment of adsorption and adhesion of proteins to polystyrene microwells by sequential enzyme-linked immunosorbent assay analysis. Anal. Biochem. 1995;225: 197-205.
17. Liedberg B, Ivarsson B, Hegg PO, Lundstam I. On the adsorption of lactoglobulin on hydrophilic gold surfaces: Studies by infrared reflection-adsorption spectroscopy and ellipsometry. J. Colloid Interface Sci. 1986;114:386-397.
18. Lok BK, Cheng YL, Robertson CR. Total internal reflection fluorescence: A technique for examining interactions of macromolecules with solid surfaces. J. Colloid Interface Sci. 1983;91:87-103.
19. Sa TJ, Lu JR, Thomas RK, Cui ZF, Penfold J. The adsorption of lysozyme at the silica-water interface: A neutron reflection study. J. Colloid Interface Sci. 1998;203:419-429.
20. Lu DR, Park K. Effect of surface hydrophobicity on the conformational changes of adsorbed fibrinogen. J. Colloid Interface Sci. 1991;144:271-281.
21. Maste MCL, Norde W, Visser AJWG. Adsorption-induced conformational changes in the serine proteinase savinase: A tryptophan fluorescence and circular dichroism study. J. Colloid Interface Sci. 1997;196:224-230.
22. Callen DC, Lowe CR. AFM studies of protein adsorption. I. Time-resolved protein adsorption to highly oriented pyrolytic graphite. J. Colloid Interface Sci. 1994;166: 102-108.
23. Norde W, Anusiem CI. Adsorption, desorption, and re-adsorption of proteins on solid surfaces. Colloids Surfaces. 1992; 66:73-80.
24. Caruso F, Furlong DN, Kingshott P. Characterization of ferritin adsorption onto gold. J. Colloid Interface Sci. 1997;186: 129-140.
25. Wahlgren M, Araebrant T, Lundstram I. The adsorption of lysozyme to hydrophilic silicon oxide surfaces: Comparison between experimental data and models for adsorption kinetics. J. Colloid Interface Sci. 1995;175:506-514.
26. Demirbas Ö, Alkan M, Demirbas A, Surface properties of catalase and casein on kaolinite and design of experiments, Microporous and Mesoporous Materials. 2013;172:151-160.
27. Van Enckevort HJ, Dass DV, Langdon AG. The adsorption of bovine serum albumin at

the stainless-steel/aqueous solution interface. J. Colloid Interface Sci. 1984;98: 138-143.
28. Alkan M, Demirbas O, Doğan M. Electrokinetic properties of sepiolite suspensions in different electrolyte media. J. Colloid and Interface Sci. 2005;281:240-248.
29. Bradford MM. A rapid and sensitive method for the quantitation of microgram quantities of protein utilizing the principle of protein-dye binding. Anal Biochem. 1976; 72:248–54.
30. Hunter RJ. Introduction to modern colloid science, Oxford University Press, New York; 2002.
31. Patwardhan AV, Ataai MM. Site accessibility and the pH dependence of the saturation capacity of a highly cross-linked matrix immobilized metal affinity chromatography of bovine serum albumin on chelating superpose. J. Chromatogr. 1997; 767:11–23.
32. Giacomelli CE, Avena MJ, De Pauli CP, Adsorption of bovine serum albumin onto TiO2 particles. J. Colloid Interf. Sci. 1997; 188:387–395.
33. Shi QH, Tian Y, Dong XY, Bai S, Sun Y. Chitosan-coated silica beads as immobilized metal affinity support for protein adsorption. Biochemical Engineering J. 2003;16:317-322.
34. Sharma S, Agarwal GP. Interactions of proteins with immobilized metal ions: Role of Ionic Strength and pH. J. Colloid Interf. Sci. 2001;243:61–72.
35. Barroug A, Lernoux E, Lemaitre J, Rouxhet PG. Adsorption of catalase on hydroxyapatite. J. Colloid Interf. Sci. 1998; 208:147-152.
36. Lu CF, Nadarajah A, Chittur KA. A comprehensive model of multiprotein adsorption on surfaces. J. Colloid Interf. Sci. 1994;168:161.
37. Giacomelli CE, Maria GEG, Bremer Norde W. ATR-FTIR study of IgG adsorbed on different silica surfaces. J. Colloid Interf. Sci. 1999;220:13–23.
38. Langmuir I. The adsorption of gases on plane surfaces of glass, mica and platinum. J. Am. Chem. Soc. 1918;40: 1361–1403.
39. Freundlich H. Adsorption in solution. Phys. Chem. 1906;57:384–410.
40. Lagergren S. Zur theorie der sogenannten adsorption gelöster stoffe. Kungliga Svenska Vetenskapsakademiens. Handlingar. 1898;4(4)1–39.
41. Ho YS, McKay G, Pseudo-second order model for sorption processes. Process Biochemistry. 1999;34(5):451-465.
42. Laidler KJ, Meiser JH. Physical chemistry, Houghton Mifflin, New York. 1999;852.
43. Michaelis L, Menten ML, Die Kinetik der Invertinwirkung. Biochem. Z. 1913;49:333–369.

Peer-review history:
The peer review history for this paper can be accessed here:
http://sciencedomain.org/review-history/17228